Properties of a new 4-imidazolyl derivative of a 14-membered tetraazamacrocyclic chelating agent†‡

Rute M. Nunes,[a] Rita Delgado,*[a,b] M. Fátima Cabral,[c] Judite Costa,[c] Paula Brandão,[d] Vítor Félix[d] and Brian J. Goodfellow[d]

Received 3rd July 2007, Accepted 17th August 2007
First published as an Advance Article on the web 7th September 2007
DOI: 10.1039/b710122h

A new bis-*N*,*N*′-(5-methylimidazol-4-ylmethyl) derivative of a 14-membered tetraazamacrocycle, L^1, has been synthesized. The protonation constants of this compound and the stability constants of its complexes with divalent first-row transition metal ions and Fe^{3+} were determined at 298.2 K in aqueous 0.10 mol dm^{-3} KNO_3. Compound L^1 exhibits high overall basicity, which is mainly conferred by the imidazolyl groups. The complexes of the divalent first row-transition metal ions of L^1 follow the Irving–Williams order of stability with the maximum for Cu^{2+} as expected, but a steep fall of constants is verified for the Mn^{2+}, Fe^{2+} and Co^{2+}, in one side, and for the Zn^{2+} complexes, in the other side. Additionally, L^1 shows a large affinity for Fe^{3+}, and the relative stability constants for its Cd^{2+} and Pb^{2+} complexes indicate that L^1 may be useful for the complexometric determination of these two toxic metal ions in solutions containing both metal ions. These studies together with NMR, UV-vis and EPR spectroscopic data indicated the presence of mononuclear complexes, which adopt distorted pyramidal or octahedral geometries depending on the metal centre. The X-ray crystal structure of $[Cu(HL^1)](PF_6)_2(NO_3)\cdot H_2O$ showed that the coordination sphere of the copper centre can be described as a distorted square pyramid with the basal plane defined by three nitrogen donors of the macrocycle backbone and one nitrogen atom from one imidazolyl pendant arm. The apical position is occupied by the nitrogen atom of the macrocycle *trans* to the pyridine ring. To achieve this coordination environment, the macrocycle is folded along the axis defined by the two N atoms contiguous to the pyridine ring. The free methylimidazolyl arm points away from the metal centre leading to an intramolecular Cu ··· N distance of 5.155(1) Å.

Introduction

The imidazole ring, in histidine, behaves as a ligand toward transition metal ions in a variety of biologically important molecules. The metalloproteins plastocyanin, azurin and hemocyanin, and the metalloenzyme carbonic anhydrase (CA) contain active centres with a histidine side chain coordinated to copper(II) and to zinc(II) ions, respectively.[1–3] In CA, a zinc(II) atom bound to an imidazolyl anion has been proposed to account for the catalytic mechanism, proton dissociation ($pK_a \approx 7$) is assigned to the HIm ⇄ Im^- equilibrium as a result of the coordination to zinc(II).[4] Histidine is also present at the active site of the biological oxygen carriers, hemoglobin and myoglobin, and the reactions of dioxygen with cobalt complexes of histidine and peptides containing histidine have been extensively studied.[5]

Model compounds containing imidazolyl moieties have been used to mimic the binding sites and the catalytic activity of such enzymes. In the last two decades some macrocyclic compounds functionalized with methylimidazolyl groups as appended arms have been synthesized and studied in this way. These include diazamacrocycles (1,5-diazacyclooctane),[6,7] triazamacrocycles (1,4,7-triazacyclononane and 1,5,9-triazacyclododecane)[8–12] and 1,4,7,10-tetraazacyclododecane (cyclen).[13–15] Cyclam (1,4,8,11-tetraazamacrocycle)[16] and 1,5,9-triazacyclododecane[4] functionalized with imidazole groups appended to the backbone were also studied.

In the present work a 14-membered tetraazamacrocycle containing pyridine with two appended methylimidazol-4-ylmethyl groups (L^1, see Scheme 1) was synthesized and its ability to coordinate metal ions was evaluated in aqueous solution. The ligand has imidazolyl groups tethered at the 4-position as in histidine, and not at the 2-position as is the case in most of the synthetic derivatives previously studied, see Scheme 1.

Results and discussion

Synthesis of the macrocycle

The compound L^1 was prepared in good yield by the reaction of the parent tetraazamacrocycle, L^2, with 4-methyl-5-imidazolecarboxaldehyde in a 1 : 2 molar ratio. The resulting Schiff base was reduced with sodium cyanoborohydride.[17] We found that

[a]*Instituto de Tecnologia Química e Biológica, UNL, Apartado 127, 2781-901, Oeiras, Portugal. E-mail: delgado@itqb.unl.pt; Fax: +351-214 41 12 77; Tel: +351-214 46 97 37/8*
[b]*Instituto Superior Técnico, Av. Rovisco Pais, 1049-001, Lisboa, Portugal*
[c]*Centro de Estudos de Ciências Farmacêuticas, Fac. de Farmácia de Lisboa, Av. Prof. Gama Pinto, 1649-003, Lisboa, Portugal*
[d]*Departamento Química, CICECO, Universidade de Aveiro, 3810-193, Aveiro, Portugal*

† CCDC reference number 652836. For crystallographic data in CIF or other electronic format see DOI: 10.1039/b710122h

‡ Electronic supplementary information (ESI) available: Tables S1–S2. See DOI: 10.1039/b710122h

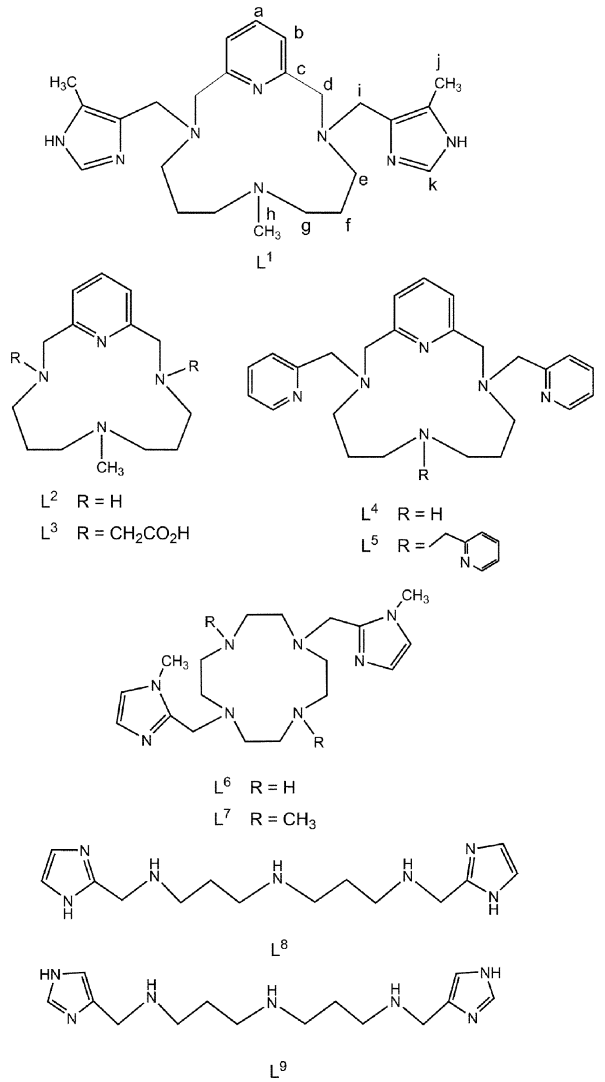

Scheme 1

the condensation of 5-chloromethyl-4-methylimidazole with the parent macrocycle under several experimental conditions, using different bases and solvents, did not yield the desired compound. This procedure, the usual route to append 2-methylimidazolyl groups to primary or secondary amines,[6,8,10,12,13] does not appear to work when binding 4-methylimidazolyl arms to the same amines.

Acid–base behaviour

The acid–base reactions of L^1 were studied in aqueous solution by potentiometric methods at 298.2 K and 0.10 mol dm^{-3} KNO_3. The determined protonation constants are collected in Table 1 together with the values for other related compounds for comparison. Of the six basic centres of the molecule only five constants could be determined by the technique used. The log K_6^H value should be <2 and it is not significant for the following studies.

The first two constants correspond to the protonation of two amine groups of the macrocycle, as also found for L^2–L^5 and other related compounds.[18–21] The first constant is as expected for a secondary amine, while the second is much lower due to the repulsion of ammonium groups at short distance and to the effect of substituents.[18–21] The third constant is a typical value for the protonation of an imidazolyl group appended to a non-protonated amine,[5,13,22] while the lower values of the fourth and fifth constants can be attributed to the protonation of the second imidazolyl group, which is bound to a protonated amine, or to the third nitrogen of the macrocycle, or certainly to the simultaneous protonation of both centres.

The difference of 1.68 units between log K_2 of L^4 and L^1 can be explained by the stronger electron-withdrawing effect of the bound methylpyridinyl groups in L^4 compared to the methylimidazolyl groups in L^1. However the values are of the same order of magnitude as those for L^6 and L^7, the differences can be assigned to the different size of the macrocycle and to the position at which the imidazolyl groups are bound to the macrocycle.

Compond L^1 exhibits higher overall basicity than that of L^3 and L^4, and is of the order of that for L^6–L^9,[5,13] which is due to the high basicity of the imidazolyl groups. The similarity between the values of L^1 and the linear compounds, L^8 and L^9, is also apparent in Table 1, the main differences are verified for K_4^H and K_5^H, for which L^1 presents lower values due to the electrostatic effects of the closer ammonium positive charges in the macrocyclic cavity of this compound.

Metal complexes studies

Stability constants

The stability constants of L^1 with K^+, Fe^{3+}, Cd^{2+}, Pb^{2+}, and the divalent first-row transition metal ions were determined at 298.2 K and in aqueous 0.10 mol dm^{-3} KNO_3. The results are collected in Table 2 (in Table S1 of ESI‡ were listed the data of related compounds for comparison). The potentiometric titration curves

Table 1 Protonation constants (log K_i^H) for L^1 and for other related ligands for comparison; $T = 298.2 \pm 0.2$ K and $I = 0.10 \pm 0.01$ mol dm^{-3} in KNO_3

Reaction equilibrium	L^{1a}	L^{3b}	L^{4c}	L^{6d}	L^{7d}	L^{8e}	L^{9e}
$L + H^+ \rightleftharpoons HL$	9.95(1)	10.72	10.65	9.55	11.47	9.76	10.12
$HL + H^+ \rightleftharpoons H_2L$	7.43(1)	7.74	5.75	8.1	8.28	7.22	8.62
$H_2L + H^+ \rightleftharpoons H_3L$	6.16(1)	4.05	3.29	5.9	5.29	6.51	7.36
$H_3L + H^+ \rightleftharpoons H_4L$	3.56(1)	1.8	1.7	3.8	3.42	3.92	4.51
$H_4L + H^+ \rightleftharpoons H_5L$	2.00(4)	—	< 0.5	—	—	3.29	3.82
$L + 4H^+ \rightleftharpoons H_4L$	27.10	24.31	21.39	27.35	28.46	27.41	30.61
$L + 5H^+ \rightleftharpoons H_5L$	29.10	—	< 21.89	—	—	—	—

[a] Values in parentheses are standard deviations on the last significant figure. [b] $I = 0.10$ mol dm^{-3} in NMe_4NO_3, ref. 18. [c] $I = 0.10$ mol dm^{-3} in NMe_4NO_3, ref. 19. [d] $I = 0.15$ mol dm^{-3} in $NaClO_4$, ref. 13. [e] $I = 0.10$ mol dm^{-3} in KNO_3, ref. 5.

Table 2 Stability constants (log units) of the complexes of L^1 with selected metal ions; $T = 298.2$ K and $I = 0.10$ mol dm^{-3} in KNO_3

Equilibrium reaction	$L = L^1$[a]
$K^+ + L \rightleftharpoons [KL]^+$	1.86(4)
$Mn^{2+} + L \rightleftharpoons [MnL]^{2+}$	7.95(1)
$[MnL]^{2+} + H^+ \rightleftharpoons [M(HL)]^{3+}$	6.09(4)
$Fe^{2+} + L \rightleftharpoons [FeL]^{2+}$	9.73(2)
$[FeL]^{2+} + H^+ \rightleftharpoons [Fe(HL)]^{3+}$	6.06(4)
$Co^{2+} + L \rightleftharpoons [CoL]^{2+}$	12.77(5)
$[CoL]^{2+} + H^+ \rightleftharpoons [Co(HL)]^{3+}$	5.73(3)
$[CoHL]^{3+} + H^+ \rightleftharpoons [Co(H_2L)]^{4+}$	3.88(5)
$Ni^{2+} + L \rightleftharpoons [NiL]^{2+}$	16.97(2)
$[NiL]^{2+} + H^+ \rightleftharpoons [Ni(HL)]^{3+}$	3.79(2)
$[NiHL]^{3+} + H^+ \rightleftharpoons [Ni(H_2L)]^{4+}$	2.64(2)
$Cu^{2+} + L \rightleftharpoons [CuL]^{2+}$	20.70(4)
$[CuL]^{2+} + H^+ \rightleftharpoons [Cu(HL)]^{3+}$	4.99(5)
$[CuL]^{2+} \rightleftharpoons [ML(OH)]^+ + H^+$	−11.09(6)
$Zn^{2+} + L \rightleftharpoons [ZnL]^{2+}$	14.28(5)
$[ZnL]^{2+} + H^+ \rightleftharpoons [Zn(HL)]^{3+}$	5.84(2)
$[ZnHL]^{3+} + H^+ \rightleftharpoons [Zn(H_2L)]^{4+}$	3.44(3)
$[ZnL]^{2+} \rightleftharpoons [ZnL(OH)]^+ + H^+$	−10.64(8)
$Cd^{2+} + L \rightleftharpoons [CdL]^{2+}$	14.67(1)
$[CdL]^{2+} + H^+ \rightleftharpoons [Cd(HL)]^{3+}$	4.99(2)
$[CdHL]^{3+} + H^+ \rightleftharpoons [Cd(H_2L)]^{4+}$	3.55(5)
$[CdL]^{2+} \rightleftharpoons [CdL(OH)]^+ + H^+$	−10.13(6)
$Pb^{2+} + L \rightleftharpoons [PbL]^{2+}$	8.93(1)
$[PbL]^{2+} + H^+ \rightleftharpoons [Pb(HL)]^{3+}$	6.35(2)
$[PbL]^{2+} \rightleftharpoons [PbL(OH)]^+ + H^+$	−11.04(3)
$Fe^{3+} + L \rightleftharpoons [FeL]^{3+}$	20.18(4)
$[FeL]^{3+} + H^+ \rightleftharpoons [Fe(HL)]^{4+}$	3.44(5)

[a] Values in parentheses are standard deviations on the last significant figure.

of L^1 alone and in M–L^1 (1 : 1) mixtures *versus* a (number of moles of KOH per mole of L^1) with most of the metal ions are shown in Fig. 1.

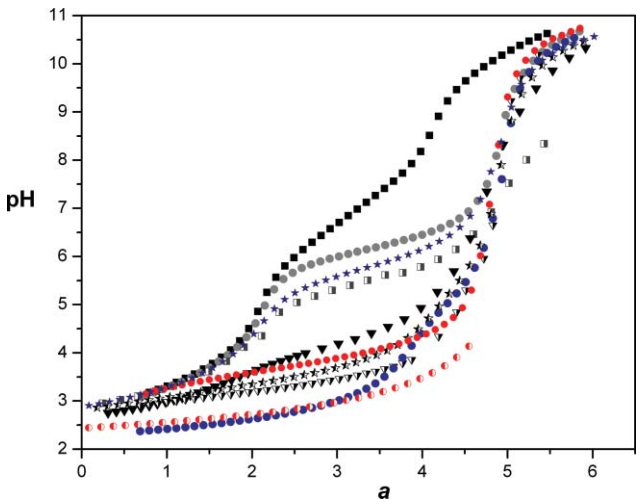

Fig. 1 Potentiometric titration curves of L^1 alone (■) and in M–L^1 (1 : 1) mixtures in function of *a* for the following metal ions: M = Fe^{3+} (red and white ◐), Mn^{2+} (grey ●), Fe^{2+} (◨), Co^{2+} (▼), Ni^{2+} (▽), Cu^{2+} (blue ●), Zn^{2+} (half-filled star), Cd^{2+} (red ●), Pb^{2+} (blue ⋆). The *a* value is the number of moles of base per mole of L^1.

Only mononuclear species, ML^1, $M(H_iL^1)$ (i = 1, 2) and $ML^1(OH)$, were found in solution for the complexes of L^1 with the metal ions studied. In some cases the $M(H_2L^1)$ species was not formed, and for Mn^{2+}, $Fe^{2+,3+}$, Co^{2+} and Ni^{2+} it was impossible to determine the constants for the formation of the hydroxo-complexes, because precipitation occurred or the kinetics of the reaction was too slow for the technique used. We checked for the formation of other species, but found none under our experimental conditions. In all cases the proposed model was accepted by the HYPERQUAD program[23] using all data points from all titration curves, converging with good statistical parameters.

$M(HL^1)$ species were found for all the metal ions studied and the stability constant extents from 3.44 (in log units) for Fe^{3+} to 6.35 for Pb^{2+}. The values for most of the complexes are slightly lower than the log K_3^H of L^1 due to the electrostatic effect of the metal ion. For the Ni^{2+} and Fe^{3+} the corresponding $K_{M(HL)}$ values are very small, which implies the coordination of both arms to these metal ions at very low pH. This is not unusual as these two metal ions in general prefer to adopt octahedral geometries. On the other hand, for the Pb^{2+} complex log $K_{M(HL)}$ > log K_3^H, which implies that the proton of the $Pb(HL^1)$ species is bound to one of the amines of the macrocycle. As the macrocycle is almost planar in the N–N_{py}–N moiety, it should fold by the two nitrogen atoms contiguous to the pyridine ring and the proton located in the amine opposite to the pyridine one. This is a common way of folding for this macrocycle, see the X-ray structure section below. Whether this type of conformation is present in complexes with Mn^{2+}, Fe^{2+}, Co^{2+} and Zn^{2+}, or even with Cu^{2+} and Cd^{2+}, cannot be determined based on potentiometric results alone.

The complexes of the divalent first row-transition metal ions of L^1 follow the Irving–Williams order of stability (Table 2). The maximum K_{ML} value was obtained for Cu^{2+} as expected, however a steep reduction for the constants for Co^{2+}, Fe^{2+} and Mn^{2+} on one side, and for the Zn^{2+} complexes on the other side, is observed. Additionally the stability constant of the CdL^1 complex is relatively high while that for Pb^{2+} is 5.74 log units lower, indicating that L^1 may be a useful ligand for the complexometric determination of these two toxic metal ions in solutions containing both. The Cd^{2+} ion will be complexed first followed by the Pb^{2+} ion. If only cadmium needs to be determined in presence of large amount of lead (up to 50 times), ligand L^1 can be used at pH 7. For a sample containing 0.05 mmol of Cd^{2+} and 2.50 mmol of Pb^{2+} in 20.0 cm^3 of aqueous solution at pH 7.0 the amount of $[CdL^1]^{2+}$ will be 2.2 × 10^{-3} mol dm^{-3} and that of $[PbL^1]^{2+}$ will be 1.9 × 10^{-5} mol dm^{-3} (see Fig. 2).

As expected the complexes of the linear ligands, L^8 and L^9, exhibit lower thermodynamic stability constants when compared with those of L^1. The comparison of constants for the three macrocyclic compounds L^1, L^3 and L^4 (Table S1‡) shows that all the three compounds exhibit similar complexometric behaviour in solution. However L^1 and L^3 have a larger affinity for Fe^{3+} than L^4, and L^1 exhibits the lowest K_{ML} value for Pb^{2+}. These conclusions are valid when the differences in the overall basicity of the various ligands are taken into account using pM = −log [M] values at physiological pH,[18,19] see Table 3.

Crystal structure of the copper(II) complex

The crystal structure is built up from an asymmetric unit composed of $[Cu(HL^1)]^{3+}$, one water solvent molecule and three counterions, two PF_6^- and one NO_3^-. The molecular structure of the cation complex is shown in Fig. 3 with the labelling scheme adopted, while selected bond distances and angles are give in Table 4. The

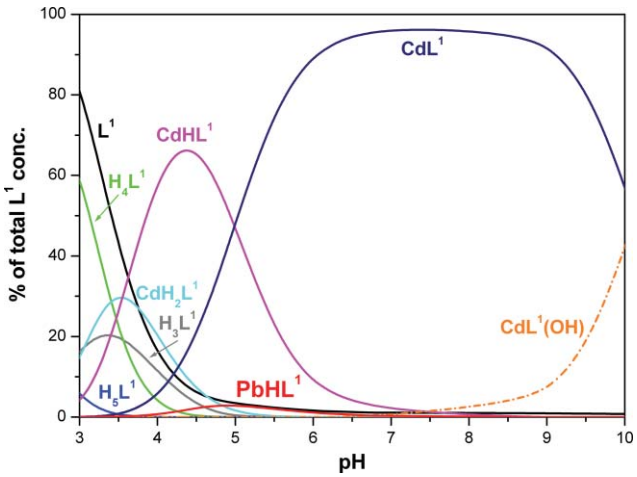

Fig. 2 Species distribution curves for an aqueous solution containing Cd^{2+}, Pb^{2+} and L^1 at a molar ratio of 1 : 5 : 1. Percentages relative to the total amount of L^1 at an initial value of 2.5×10^{-3} mol dm^{-3}.

Table 3 pM values for first-row transition metal ions, Cd^{2+}, Pb^{2+} and Fe^{3+} complexes of L^1 and $L^{3,4,8,9}$[a]

Ligand	L^1	L^3	L^4	L^8	L^9
pMn	5.43	—	—	—	—
pFe^{2+}	6.88	—	—	—	—
pCo	9.90	10.58	10.24	8.95	7.13
pNi	14.09	12.77	13.68	12.41	10.70
pCu	17.82	17.79	16.87	15.86	14.73
pZn	11.71	10.38	11.39	9.30	7.60
pCd	11.79	—	11.59	—	—
pPb	6.15	7.08	7.43	—	—
pFe^{3+}	17.30	16.82	12.61	—	—

[a] Values calculated for 100% excess of free ligand at physiological conditions, pH = 7.4; $C_M = 1.0 \times 10^{-5}$ mol dm^{-3}, $C_L = 2.0 \times 10^{-5}$ mol dm^{-3}, using the Hyss program.[24]

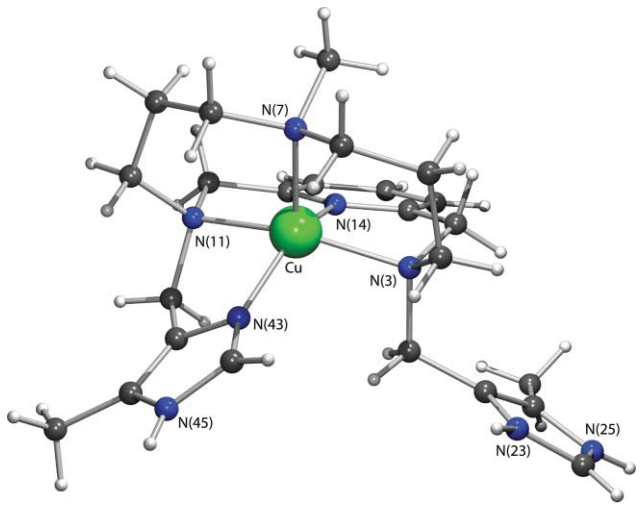

Fig. 3 Molecular diagram structure of $[Cu(HL^1)]^{3+}$ with the labelling scheme adopted.

copper(II) coordination sphere can be described as a distorted square pyramid with the basal coordination plane defined by three nitrogen donors [N(11), N(14) and N(3)] and one nitrogen atom [N(43)] from one imidazolyl pendant arm. The apical position is occupied by the nitrogen atom N(7) *trans* to the pyridine ring. To achieve this coordination environment, the macrocycle is folded along the axis defined by the atoms N(11) and N(3) giving a dihedral angle between the planes N(3),N(7),N(11) and N(3),N(11),N(14) of 76.55(4)°. The free methylimidazolyl pendant arm is further away from the metal centre leading to an intramolecular Cu···N(23) distance of 5.155(1) Å. The copper is located 0.4911(5) Å above this N_4 coordination plane towards the apical nitrogen giving a Cu–N(7) distance of 2.1353(10) Å, which is consistent with the distance of the nitrogen N(7) to the plane of 2.626(1) Å. However a trigonal distortion is apparent from two *trans* N–Cu–N angles, giving a τ parameter of 0.27.

Table 4 Selected bond distances and angles for $[Cu(HL^1)]^{3+}$

Bond distances/Å			
Cu–N(3)	2.0768(9)	Cu–N(7)	2.1353(10)
Cu–N(11)	2.0766(1)	Cu–N(14)	1.9444(9)
Cu–N(43)	1.9903(9)		
C(22)–C(26)	1.3651(15)	C(22)–N(23)	1.3880(14)
C(24)–N(23)	1.3265(15)	C(24)–N(25)	1.3298(16)
C(26)–N(25)	1.3822(14)		
C(42)–C(46)	1.3616(16)	C(42)–N(43)	1.3884(14)
C(44)–N(43)	1.3288(15)	C(44)–N(45)	1.3434(15)
C(46)–N(45)	1.3790(16)		
Bond angles/°			
N(14)–Cu–N(43)	141.77(4)	N(14)–Cu–N(11)	81.97(3)
N(43)–Cu–N(11)	83.56(3)	N(14)–Cu–N(3)	81.88(4)
N(43)–Cu–N(3)	100.02(4)	N(11)–Cu–N(3)	157.78(3)
N(14)–Cu–N(7)	108.50(4)	N(43)–Cu–N(7)	108.81(4)
N(11)–Cu–N(7)	100.24(3)	N(3)–Cu–N(7)	99.30(4)

This geometric arrangement compares well with that found for the copper complex of L^5.[19] The complex $[CuL^5]^{2+}$ displays a distorted square pyramidal coordination with one nitrogen atom from one pyridylmethyl pendant arm and the nitrogen *trans* to the pyridine ring of the macrocyclic backbone occupying the basal and the apical positions, respectively. The second pendant arm is away from the metal centre leading to a Cu···N distance of 5.205(9) Å, as also found in $[Cu(HL^1)]^{3+}$. By contrast, the third arm of L^5 is pointing toward the metal centre with the nitrogen donor at 3.304(11) Å from the metal. The Cu–N distances are similar in these two complexes and follow the same pattern. As would be expected, in both complexes the Cu–N apical distances are longer than the equatorial distances.

The C–N and C–C distances for both imidazole rings, listed in Table 4, show that three consecutive distances are longer than the remaining two. In addition, this distance pattern is similar in both five-membered rings and is consistent with either the protonation or the coordination of these pendant arms.

In the crystal structure of $[Cu(HL^1)]^{3+}$, the complex cation and NO_3^- counterions are assembled through N–H···O hydrogen bonding interactions, forming 1-D dimensional chain as shown in Fig. 4. Two neighbour $[Cu(HL^1)]^{3+}$ ions are bridged thorough three concomitant hydrogen bonds between the two N–H groups from their free methylimidazolyl pendant arms and the NO_3^- anion with H···O distances of 1.96, 2.35 and 2.28 Å. These interactions are complemented by a N–H···O hydrogen bond between N–H group from the coordinated methylimidazolyl arm of a third $[Cu(HL^1)]^{3+}$ and the nitrate anion with a H···O distance of 2.01 Å.

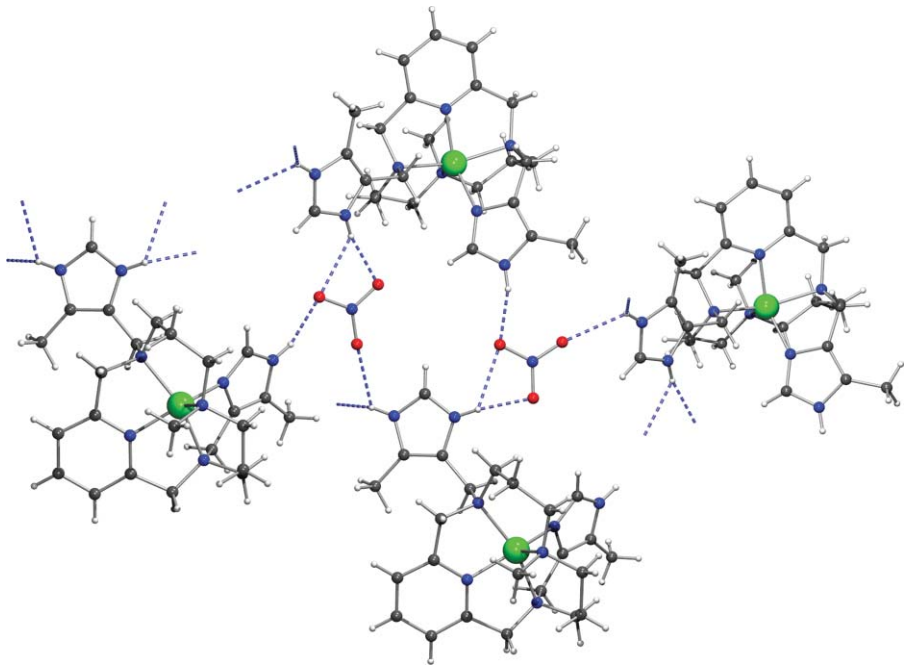

Fig. 4 Crystal packing diagram of $[Cu(HL^1)].(PF_6)_2.NO_3.H_2O$ showing the 1-D dimensional network of N–H · · · O hydrogen bonds. The PF_6^- anions and water molecules were omitted for clarity.

In addition, N–H · · · O and N–H · · · F, the O from water solvent molecule and the F from PF_6^- anions, respectively, were also found in the crystal structure. The dimensions of all hydrogen bonds are given in Table 5.

Spectroscopic studies

NMR spectroscopic data of metal complexes in solution

Suitable crystals for X-ray diffraction of the Zn^{2+}, Cd^{2+} and Pb^{2+} complexes of L^1 could not be obtained, however the ^1H NMR spectra of these complexes were acquired in D_2O (Table 6) and gave some insight into their structures in solution. The spectral assignments, made by TOCSY, ROESY and HMQC experiments, correspond to the labelling shown in Scheme 1.

In the spectrum of the $[CdL^1]^{2+}$ complex, the aromatic protons H_a (7.92) and H_b (7.36) were assigned *via* their TOCSY spin system and *via* a NOE between H_b and $H_d/H_{d'}$ (3.95, 3.85). The remaining aromatic proton was assigned to H_k (7.68). The most intense singlet was assigned to H_j (2.24) and the remaining singlet to H_h (2.51). Protons $H_i/H_{i'}$ were assigned *via* an NOE with H_j and protons $H_g/H_{g'}$ were assigned *via* an NOE with H_h. Protons $H_e/H_{e'}$ were assigned through NOEs with protons $H_i/H_{i'}$ and the remaining protons were assigned to $H_f/H_{f'}$.

In order to probe whether the pendant imidazolyl arms (containing protons H_i, H_j and H_k) were bound to the cadmium central atom giving an octahedral complex, a low temperature ROESY spectrum was recorded at 285 K. A molecular model of an octahedral complex places protons H_k approximately 3 Å from protons $H_e/H_{e'}$, $H_d/H_{d'}$ and $H_g/H_{g'}$ which should result in NOESY cross peaks being seen. At 285 K (and at 300 K) no NOEs were observed suggesting the pendant arm is not coordinated for this metal in solution. To confirm this finding a ^1H-^{113}Cd HSQC experiment was carried out at 290 K. Here cross peaks between the ^{113}Cd resonance (97.3 ppm) and protons H_a (weak), H_k (med), H_b (str), $H_d/H_{d'}$ (str), $H_i/H_{i'}$ (med), $H_e/H_{e'}$ (med), H_g (str) and H_j (med) were seen. The presence of cross peaks between the Cd atom and protons H_j and H_k suggests that there is, in fact, an interaction between the pendant imidazolyl arms and the central Cd atom. However, the interaction must be fast on the chemical shift time scale at these temperatures.

Table 5 Dimensions of the hydrogen bonds for $[Cu(HL^1)]^{3+}$

A = acceptor; D = donor	H · · · A/Å	D · · · A/Å	D · · · H · · · A/°
N(23)–H(23) · · · O(81) [−x + 1, y + 1/2, −z + 1/2]	1.96	2.779(2)	159
N(23)–H(23) · · · O(82) [−x + 1, y + 1/2, −z + 1/2]	2.35	2.932(2)	125
N(25)–H(25) · · · O(100) [x, y + 1, z]	2.28	2.977(2)	138
N(45)–H(45) · · · O(82) [x, y + 1, z]	2.01	2.842(2)	163
N(45)–H(45) · · · O(83)	2.62	3.340(2)	142
O(100)–H(101) · · · F(24) [x, −y + 1/2, z − 1/2]	2.31(2)	3.117(2)	169(2)
O(100)–H(101) · · · F(22) [x, −y + 1/2, z − 1/2]	2.45(2)	3.092(2)	136(2)
O(100)–H(101) · · · F(23) [x, −y + 1/2, z −1/2]	2.48(2)	3.066(2)	130(2)
O(100)–H(102) · · · F(15) [x, −y + 1/, −z]	2.44(3)	3.009(2)	127(2)

Table 6 ^{1}H NMR chemical shifts found for L^1 and its Zn^{2+} (300 K), Cd^{2+} (285 K) and Pb^{2+} (285 K) complexes

Species	H_a (t)	H_b (d)	H_d	H_e	H_f	H_g	H_h	H_i	H_j	H_k
L^1	7.93	7.32	3.90	3.20	2.00	2.90	2.87	3.75	2.28	7.84
ZnL^1	7.97	7.38	4.31 (d); 4.00 (t)	3.13	1.82; 2.39	3.12; 2.68	2.22	3.80; 4.00	2.21	7.56
CdL^1	7.92	7.36	3.95 (d); 3.85 (d)	2.75	1.87; 2.11	2.90; 2.54	2.51	4.05; 3.64	2.24	7.68
PbL^1	7.87	7.34	4.18 (d)	2.98; 2.82	2.05; 2.10	3.10; 2.40	2.23	4.22; 3.85	2.23	7.48

UV-vis of the nickel(II), cobalt(II) and copper(II) complexes

The UV-vis-NIR data for the Co^{2+}, Ni^{2+} and Cu^{2+} complexes of L^1 in water solution are collected in Table S2.‡ The electronic spectrum of the pink cobalt complex solution exhibits three principal bands at 1167, 506 and 260 nm and two shoulders, indicating a six coordinate tetragonally distorted symmetry high-spin Co(II) species. The band at 506 nm is more intense than predicted for forbidden transitions in O_h complexes, and the value of the magnetic moment of 4.9 MB although within the range for a six-coordinate complex it is also within the expected range for five-coordinate species. However, five-coordinate chromophores would present a weak absorption between 830 to 670 nm,[25–27] and the $[CoL^1]^{2+}$ complex does not exhibit absorptions in this region. The electronic spectrum observed for the green $[NiL^1]^{2+}$ complex shows three well defined bands at 1072, 769 and 572 nm of low intensity, characteristic of a high-spin six-coordinate complex. The magnetic moment of 3.1 BM also falls in the range usually observed for high-spin six coordinate Ni^{2+} environments and is characteristic of a tetragonally distorted octahedral symmetry.[28] The $[CuL^1]^{2+}$ complex exhibits a broad band in the visible region with λ_{max} at 639 nm due to the copper d–d transitions, an intense band in the UV region and a small broad band in the near-IR region, see Table S2.‡

X-band EPR spectra of the manganese(II), cobalt(II) and copper(II) complexes

The X-band EPR spectra of the $[MnL^1]^{2+}$ complex in aqueous and in H_2O : DMSO 1 : 1 solutions were recorded at pH 7.67 and 9 K. The spectra are typical of a high-spin d^5 configuration (^{55}Mn, $S = 5/2$, $I = 5/2$) showing, as the main resonance at $g = 2.036$, a nuclear hyperfine structure of a well resolved sextet, due to the hyperfine interaction between the unpaired electrons and ^{55}Mn, with hyperfine splitting constant A of 98.21 G, shown in Fig. 5. In addition, between every adjacent pair of these six "allowed" hyperfine lines ($\Delta M = \pm 1$, $\Delta m = 0$), a pair of relatively weak "forbidden" hyperfine transitions ($\Delta M = \pm 1$, $\Delta m = \pm 1$) are also observed (M = electron spin quantum number and m = nuclear spin quantum number), see Fig. 5(b). The average separation of the "forbidden" hyperfine doublets in the spectrum is 27.3 G. The experimental results also show at half-field a weaker resonance at $g = 4.8$, see Fig. 5(a).[29–34] This resonance is due to first-order admixtures to the wavefunctions arising from $\Delta M = \pm 1$ off-diagonal elements of D, when H is not parallel to the D axis, the dipole selection rules permit transitions $\Delta M = \pm 2$, $\Delta m = \pm 0$. The large hyperfine splitting reveals that the Mn^{2+} ion is strongly ionic.[29] The observed values of g and A are consistent with a mononuclear Mn(II) complex with octahedral symmetry.[35–38]

The X-band EPR spectra of the Co^{2+} complex were recorded at 8, 10 and 30 K. They show as a principal feature a broad and intense band centred at about 1000 G and completely anisotropic g values, with signals corresponding to two species. The apparent g values are $g_1' = 6.21$, $g_2' = 2.79$ and $g_3' = 1.6$, and no hyperfine splitting due to the interaction with the Co^{2+} nucleus ($I = 7/2$) was detected. The other species presents very similar signals at $g_1' = 7.6$, $g_2' = 3.16$ and the g_3' cannot be distinguished from that of the first species. Because of the broadness and overlapping of the bands, the g values could not be determined with good accuracy. Additionally the typical signals of a species resulting from the reaction of a cobalt(II) complex with molecular oxygen, which is a low spin species, appears at 2.3.[39,40]

The observed main signals are typical of high-spin cobalt(II) complexes ($S = 3/2$) in a rhombically distorted octahedral or square pyramidal complex, which can be interpreted by using an effective $S = 1/2$ spin Hamiltonian.[39–42] Using only the g values it is not possible to discriminate between the two stereochemistries.[41–43] However the low-intensity of the bands of the electronic spectra

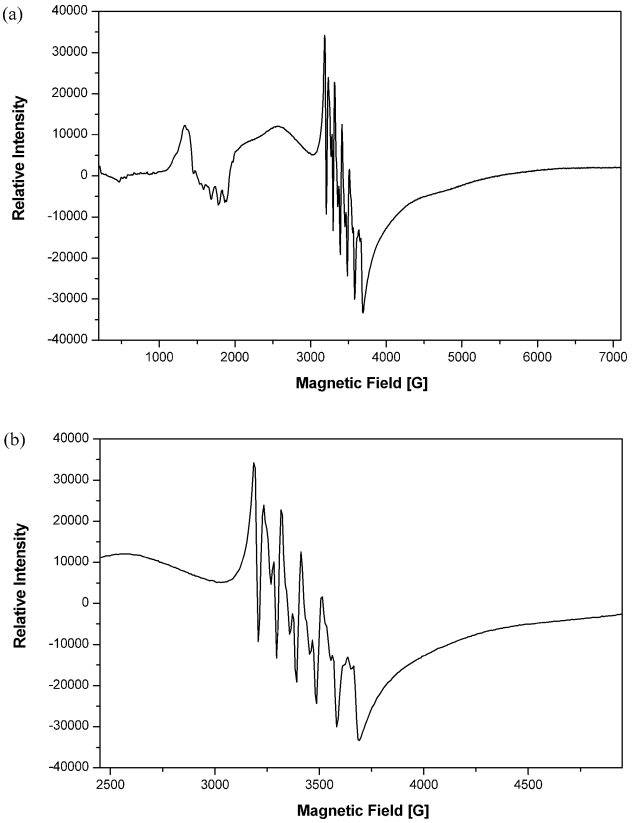

Fig. 5 (a) X-band EPR spectrum of $[MnL^1]^{2+}$ complex in H_2O : DMSO 1 : 1 solution and 8.85×10^{-4} mol dm^{-3} recorded at pH 7.67 and 9 K. (b) A fragment of the spectrum centred in the signal at $g = 2$. Microwave power of 2.0 mW, modulation amplitude of 1.0 mT and the frequency (ν) was of 9.643 GHz.

Table 7 Spectroscopic X-band EPR data for the Cu^{2+} complexes of L^1 and other similar complexes for comparison

Complex	Vis band λ_{max}/nm	EPR parameters ($A_i \times 10^4$ cm^{-1})						
		g_x	g_y	g_z	A_x	A_y	A_z	Ref.
$[CuL^1]^{2+}$	639	2.048	2.076	2.223	5.4	14.1	170.7	This work
$[CuL^2]^{2+}$	560	2.039	2.080	2.201	4.9	14.7	195.9	51
$[CuL^4]^{2+}$	661	2.036	2.086	2.220	5.7	19.7	172.6	50
$[CuL^5]^{2+}$	660	2.030	2.070	2.217	1.5	0.5	169.9	50

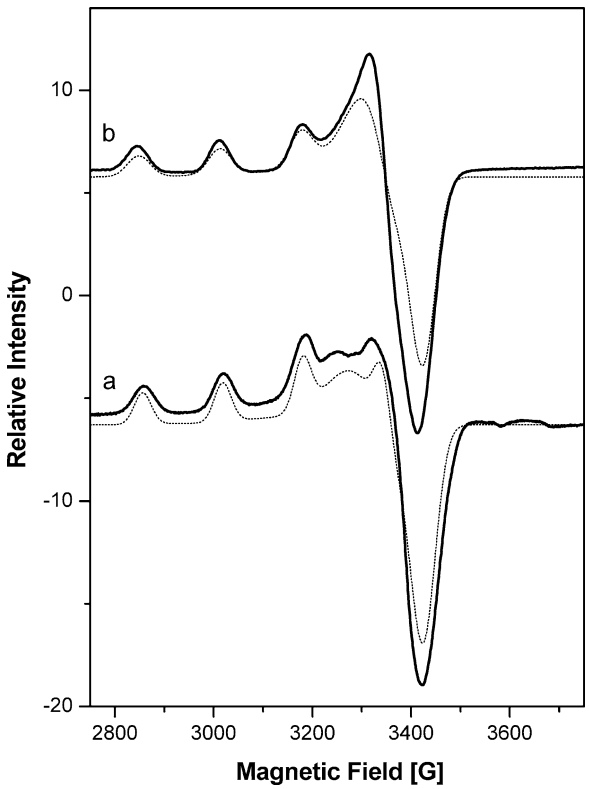

Fig. 6 X-band EPR spectra of $[CuL^1]^{2+}$ complexes: (a) in aqueous solution at pH 4.04 (1.47×10^{-2} mol dm^{-3} in 1.0 mol dm^{-3} $NaClO_4$) recorded at 14 K and (b) in DMF (1.79×10^{-3} mol dm^{-3}) recorded at 10 K. The microwave power was 2.0 mW, the modulation amplitude was 1.0 mT and the frequency (ν) was 9.644 GHz. The simulated spectra are showed below of the experimental ones as dotted lines.

and the absence of a weak band in the 830–660 nm region, led us to infer that our cobalt(II) complex adopts a distorted octahedral geometry. The relative values of g (g_1, $g_2 > g_3$) show that the axial deformation is an elongation. Distortions of the complex are the possible causes for the large rhombicity g_1–g_2 of the complex.[44,45] Spectra similar to that found for $[CoL^1]^{2+}$ are common in the literature.[39–42]

The X-band EPR spectra of the copper(II) complex were performed at 10 and 14 K, and at pH 7.04 and 4.04, and are shown in Fig. 6. They exhibit the four expected lines at low field, and no superhyperfine splitting was observed. The simulation of the spectra[46] indicated three different principal values of g, $g_z > (g_x + g_y)/2$ and the lowest $g \geq 2.04$, characteristic of mononuclear copper(II) complexes in rhombic symmetry with elongation of the axial bonds and a $d_{x^2-y^2}$ ground state. Elongated rhombic-octahedral or distorted square pyramidal stereochemistries would be consistent with these data.[47–49] The A and g values of a frozen solution of the complex are compiled in Table 7, together with those of other copper(II) complexes of ligands having the same macrocyclic framework but different pendant arms.

As expected the g_z values increase and the A_z values decrease when the planar ligand field becomes weaker or the axial ligand field becomes stronger, and this occurs with the simultaneous red-shift of the d–d absorption bands in the electronic spectra. This sequence parallels the degree of distortion from square-planar to square pyramidal (C_{4v}), and then to octahedral (O_h) or tetragonal (D_{4h}) geometries.[49,50] Accordingly the $[CuL^2]^{2+}$ complex, which adopts a square planar geometry with the metal centre located into the macrocyclic ring,[50,51] presents lower g_z, higher A_z, and the visible band is blue-shifted compared to the corresponding values for $[CuL^1]^{2+}$ and the other complexes referred in Table 7. The similarity of the EPR parameters of $[CuL^1]^{2+}$ and $[CuL^5]^{2+}$ points to the same geometric environment for the copper(II) centre of both complexes, as also found with the corresponding crystal structures, see the X-ray section.

Conclusions

The complexes of the divalent first row-transition metal ions of L^1 follow the Irving–Williams order of stability (Table 2). The maximum K_{ML} value was obtained for Cu^{2+} as expected, however a steep reduction for the constants for Co^{2+}, Fe^{2+} and Mn^{2+} on one side, and for the Zn^{2+} complexes on the other side, was seen. Additionally the stability constant of the CdL^1 complex is relatively high while that for Pb^{2+} is 5.74 log units lower, indicating that L^1 may be a useful ligand for the complexometric determination of these two toxic metal ions in solutions containing both. Titrations for Cd^{2+} can be carried out in the presence of a 50-fold excess of Pb^{2+} at pH 7. A remarkably high stability constant for the $[FeL^1]^{3+}$ complex was also found.

The structural studies of several complexes suggested that the metal centres can easily adopt a square-pyramidal or octahedral geometry, with one or two imidazolyl arms involved in the coordination to the metal centre.

The present work has shown the properties of the compound L^1 and several of its divalent complexes that exhibit interested spectroscopic features, and some remarkable differences of stability constants between several complexes allowing to predict possible analytical applications.

Experimental

Microanalyses were carried out by the ITQB Microanalytical Service. Melting points were determined with a Büchi 530 Melting Point apparatus. Magnetic moments of the cobalt(II), nickel(II)

and copper(II) complexes were determined by the Evans method[52] in solution at 298 K.

Reagents

2,6-Pyridinedimethanol, 3,3′-diamine-*N*-methyldipropylamine and 4-methyl-5-imidazole-methanol hydrochloride were obtained from Aldrich. 2,6-Pyridinedicarbaldehyde and 7-methyl-3,7,11,17-tetraazabicyclo[11.3.1]heptadeca-1(17),13,15-triene (L^2) were prepared by published methods.[20] Active manganese dioxide was prepared from manganese carbonate by heating at 250 °C during 5 h. 4-Methyl-5-imidazolecarboxaldehyde was obtained from 4-methyl-5-imidazolemethanol by reaction with active manganese dioxide at rt during 3 d.[17] All the other chemicals were of reagent grade and used as supplied without further purification. Organic solvents were purified or dried by standard methods.[53]

The reference used for the ^{1}H NMR measurements in D_2O was 3-(trimethylsilyl)-propanoic acid-d_4-sodium salt and in $CDCl_3$ as the solvent itself. For ^{13}C NMR spectra 1,4-dioxane was used as internal reference.

Synthesis of 3,11-bis(4-imidazolylmethyl)-7-methyl-3,7,11,17-tetraazabicyclo[11.3.1]hepta-deca-1(17),13,15-triene, L^1

The parent macrocycle (L^2) (0.100 g, 0.402 mmol) and 4-methyl-5-imidazolecarboxaldehyde (0.186 g, 1.61 mmol) were dissolved in methanol (4 cm^3) at rt. To this solution, upon degassing by several cycles and refilling with nitrogen, sodium cyanoborohydride 95% (0.111 g, 1.77 mmol) was added. The mixture was stirred for 20 d at rt under nitrogen. At the end of this time, the solution was acidified to pH 2 with concentrated hydrochloric acid, the hydrogen gas was left to evolve, and then a white precipitate was formed which was filtered off. The filtrate was evaporated to dryness, and the yellow oil formed was dissolved in methanol (3 cm^3). The white solid formed was filtered off and the filtrate was evaporated to dryness. This procedure was repeated until the white precipitate was no longer formed. Then the solvent was removed again. The solid obtained was dissolved in HCl 6 mol dm^{-3} (15 cm^3) and the solution refluxed during 3 h at 95 °C, and then passed through an ionic exchange column (Dowex 1 × 8 in the OH^- form), using water as eluent. The fractions of basic pH were collected and evaporated to obtain a yellow oil, which was washed several times in methanol and dried *in vacuum*. The product obtained was identified as the pure desired compound. Yield: 0.286 mmol (71.2%). Mp 223–5 °C (dec.). ^{1}H NMR (D_2O, pD = 7.9): δ 1.22 (6 H, q, $NCH_2CH_2CH_2N$), 1.88 (3 H, s, NCH_3), 1.93 (4 H, t, $NCH_2CH_2CH_2N$), 1.95 (6 H, s, $imCH_3$), 2.26 (4 H, t, $NCH_2CH_2CH_2N$), 3.45 (8 H, s, CH_2py and NCH_2im), 7.02 (4, d, py), 7.49 (2 H, s, im) and 7.55 (2 H, t, py). ^{13}C NMR (D_2O): δ 9.7 ($imCH_3$), 22.5 ($NCH_2CH_2CH_2N$), 42.9 (NCH_3), 49.9 ($NCH_2CH_2CH_2N$), 51.1 ($NCH_2CH_2CH_2N$), 53.2 ($pyCH_2N$), 59.1 (NCH_2im), 123.7, 127.4, 129.3 (im), 134.4 (py), 138.0 (py) and 157.3 (py). Found: C, 60.65; H, 8.81; N, 23.89%. Calc. for $C_{24}H_{36}N_8 \cdot 2H_2O$: C, 60.99; H, 8.53; N, 23.71%.

Synthesis of the complex $[Cu(HL^1)](PF_6)_2(NO_3)$

An aqueous solution of $Cu(NO_3)_2.6H_2O$ (1.0 cm^3, 0.05 mmol) was added to a stirred solution of $H_5L^1(NO_3)_5$ (20.0 cm^3, 0.05 mmol) dissolved also in water. Then 0.018 g of NH_4PF_6 was added and the mixture stirred at 60 °C for one hour. The pH of the solution was increased to 5.5 by addition of a solution of KOH 0.1 mol dm^{-3} and the solvent was evaporated under vacuum. The residue was then taken in a minimum amount of MeOH–CH_3CN 10 : 1 (v/v). Blue crystals were formed in about two weeks by slow evaporation of the solvent at room temperature. Yield: ≈85%. Found: C, 40.56; H, 5.22; N, 17.79%. Calc. for $C_{24}H_{36}CuF_6N_9O_3P$: C, 40.77; H, 5.13; N, 17.83%.

Potentiometric measurements.

Reagents and solutions. Solutions containing approximately 0.025 mol dm^{-3} of metal ion were prepared from the nitrate salts of the metals and were titrated using standard methods. Demineralized water (Millipore/Milli-Q System) was used. Carbonate-free solutions of the titrant, KOH, were obtained, maintained and discarded as described.[18,19,50]

Equipment and work conditions. The equipment used was described previously.[18,19,50] The temperature was kept at 298.2 ± 0.1 K; atmospheric CO_2 was excluded from the cell during the titration by passing purified nitrogen across the top of the solution in the reaction cell. The ionic strength was kept at 0.10 ± 0.01 mol dm^{-3} with KNO_3.

Measurements. The [H^+] of the solutions was determined by the measurement of the electromotive force of the cell, $E = E'^\circ + Q \log [H^+] + E_j$. E'°, Q, E_j and $K_w = ([H^+][OH])$ were obtained as described previously.[18,19,50] The term pH is defined as $-\log [H^+]$. The value of K_w was found to be equal to $10^{-13.80}$ mol^2 dm^{-6}.

The potentiometric equilibrium measurements were carried out using 20.00 cm^3 of ≅2.50×10^{-3} mol dm^{-3} ligand solutions diluted to a final volume of 30.00 cm^3, in the absence of metal ions and in the presence of each metal ion with $C_M : C_L$ ratios of 1 : 2, 1 : 1 and 2 : 1. A minimum of three replicate measurements was taken.

Calculation of equilibrium constants. Protonation constants $K_i^H = [H_iL]/([H_{i-1}L] \times [H])$ were calculated by fitting the potentiometric data obtained for the free ligand to the HYPERQUAD program.[23] Stability constants of the various species formed in solution were obtained from the experimental data corresponding to the potentiometric titrations of solutions of different $C_M : C_L$ ratios, also using the HYPERQUAD program. The initial computations were obtained in the form of overall stability constants, $\beta_{M_mH_hL_l}$ values, $\beta_{M_mH_hL_l} = [M_mH_hL_l]/([M]^m \times [H]^h \times [L]^l$. Only mononuclear species, ML, MH_iL (i = 1–2) and $MH_{-1}L$ were found for most of the metal ions studied with L^1 (being $\beta_{MH_{-1}L} = \beta_{MH_hL_l} \times K_w$). Differences, in log units, between the values of protonated or hydrolysed and non-protonated constants provide the stepwise reaction constants. The species considered in a particular model were those that could be justified by the principles of coordination chemistry. The errors quoted are the standard deviations of the overall stability constants given directly by the program for the input data, which include all the experimental points of all titration curves. The standard deviations of the stepwise constants, shown in Tables 1 and 2 (and Table S1 in ESI‡), were determined by normal propagation rules.

The protonation constants of L^1 were determined from a minimum of 140 points and the stability constants were determined from a minimum of 110 and 159 points for the copper(II) and lead(II) complexes, respectively. All the reactions of L^1 with the metal ions were fast, except with Ni^{2+} and Fe^{3+}, for which

backtitrations using HNO_3 solutions as the titrant were also performed.

Spectroscopic studies. ^1H and ^{13}C NMR spectra were recorded on a Bruker CXP-300 or a Bruker DRX-500 spectrometers. Solutions of the ligands and respective complexes for the measurements ($\approx$0.01 mol dm^{-3}) in D_2O were made up and the pD was adjusted by addition of DCl or CO_2-free KOD with an Orion 420A instrument fitted with a combined Ingold 405M3 microelectrode. The $-\log [D^+]$ was measured directly in the NMR tube, after the calibration of the microelectrode with buffered aqueous solutions. The final pD was calculated from pD = pH* + 0.40.[54] The value of pH* corresponds to the reading of the pH meter previously calibrated with two standard aqueous buffers at pH 4 and 7.

The 2D ROESY spectra were acquired at 500 MHz using a 250 ms mixing time and sweep widths of 6000 Hz. Co-addition of 8 scans for each of the 512 increments in the F1 dimension was used along with TPPI detection. The [^{1}H-^{113}Cd]-HSQC spectrum was acquired at 500 MHz using sweep widths of 6000 (^{1}H) and 66500 Hz (^{113}Cd). Co-addition of 16 scans for each of the 128 increments in the F1 dimension was used along with TPPI detection. A ^{1}H-^{113}Cd coupling constant of 5 Hz was used.

Electronic spectra were recorded with a UNICAM model UV-4 and a Shimadzu model UV-3100 spectrophotometers for UV-vis and NIR ranges, respectively, using aqueous solutions of the complexes prepared by the addition of the metal ion (in the form of nitrate salt) to the ligand at the appropriate pH value, as following: (1) $[CoL^1]^{2+}$ complex (4.88×10^{-3} mol dm^{-3} for the UV-NIR region and 5.35×10^{-5} mol dm^{-3} for the UV region) were recorded at different pH values in the range 3.65 to 11.11; (2) $[NiL^1]^{2+}$ complex (1.0×10^{-2} mol dm^{-3} and 5.53×10^{-5} mol dm^{-3}) at the pH 3.03 to 10.41 pH range; (3) $[CuL^1]^{2+}$ complex (7.3×10^{-3} mol dm^{-3} and 9.43×10^{-5} mol dm^{-3}) at the 3.01 to 9.95 pH range. The spectra at different pH values exhibit only slight differences in λ_{max} by the increase of pH but they exhibit increasing intensity. Upon pH 8.09 for the cobalt, 8.66 for nickel and 9.95 for copper complexes the decrease of the intensity of the bands testifies the presence of a precipitate.

EPR spectroscopy measurements of the Mn^{2+}, Co^{2+} and Cu^{2+} complexes were recorded with a Bruker ESP 380 spectrometer equipped with continuous-flow cryostats for liquid helium or liquid nitrogen, operating at X-band. The spectra were recorded at the following conditions: $[MnL^1]^{2+}$ complex at 9 K (1.77×10^{-3} mol dm^{-3} in 1.0 mol dm^{-3} $NaClO_4$ at pH 7.67, and 8.85×10^{-4} mol dm^{-3} in H_2O : DMSO 1 : 1 solution); $[CoL^1]^{2+}$ complex (1.37×10^{-2} mol dm^{-3} in 1.0 mol dm^{-3} $NaClO_4$ at the pH 7.03) at 10, 22 and 30 K and in H_2O : DMSO 1 : 1 solution (6.85×10^{-3} mol dm^{-3}) at 8 K; $[CuL^1]^{2+}$ complex (1.47×10^{-2} mol dm^{-3} in 1.0 mol dm^{-3} $NaClO_4$ at pH 4.04) at 14 K and at 10 K (1.79×10^{-3} mol dm^{-3} in DMF).

Crystallography

Crystal data. $C_{24}H_{39}CuF_{12}N_9O_4P_2$, $M_r = 871.12$; monoclinic space group, $Z = 4$, $a = 16.7492(5)$ Å, $b = 12.6147(4)$ Å, $c = 17.2441(5)$ Å, $\beta = 110.0220(10)°$, $U = 3423.24(18)$ Å^3, $T = 296$ K, space group $P2_1/c$ (N° 14), ρ(calc) = 1.690 Mg m^{-3}, (Mo-Kα) 0.844 mm^{-1}. 95478 intensities collected, 18737 independent reflections (R_{int} of 0.0252), which were used in solution and structure refinement. The final R and R_w indices were $R_1 = 0.0390$ and $wR_2 = 0.0972$ for 13967 reflections with $I > 2\sigma(I)$ and $R_1 = 0.0624$ and $wR_2 = 0.1075$ for all hkl data.

The X-ray data were collected at room temperature on a CCD Bruker APEX II using graphite monochromatized Mo-Kα radiation ($\lambda = 0.71073$ Å) with the crystal positioned at 35 mm from the CCD and the spots were measured using a counting time of 5 s. Data reduction and empirical absorption were carried out using the SAINT-NT from Bruker aXS. The structure was solved by direct methods and by subsequent difference Fourier syntheses and refined by full matrix least squares on F^2 using the SHELX-97 system programs.[55] Anisotropic thermal parameters were used for all non-hydrogen atoms. Hydrogen atoms bonded to the carbon atoms were included in refinement in calculated positions with isotropic parameters equivalent 1.2 times those of the atom to which they are attached. Molecular diagrams presented are drawn with the graphical package software PLATON.[56]

Acknowledgements

The authors acknowledge the financial support from Fundação para a Ciência e a Tecnologia (FCT) and POCTI, with co-participation of the European Community fund FEDER (Project n. POCTI/2002/QUIM/49114).

References

1 R. J. Sundberg and R. B. Martin, *Chem. Rev.*, 1974, **74**, 471.
2 I. Bertini, C. Luchinat and A. Scozzafava, *Struct. Bonding*, 1982, **48**, 45.
3 K. Várnagy, I. Sóvágó, H. Süli-Vargha, D. Sanna and G. Micera, *J. Inorg. Biochem.*, 2000, **81**, 35.
4 E. Kimura, Y. Kurogi, M. Shionoya and M. Shiro, *Inorg. Chem.*, 1991, **30**, 4524.
5 J. H. Timmons, W. R. Harris, I. Murase and A. E. Martell, *Inorg. Chem.*, 1978, **17**, 2192.
6 X.-H. Bu, M. Du, Z.-L. Shang, R.-H. Zhang, D.-Z. Liao, M. Shionoya and T. Clifford, *Inorg. Chem.*, 2000, **39**, 4190.
7 X.-H. Bu, M. Du, L. Zhang, Z.-L. Shang, R.-H. Zhang and M. Shionoya, *J. Chem. Soc., Dalton Trans.*, 2001, 729.
8 M. Di Vaira, F. Mani and P. Stoppioni, *J. Chem. Soc., Chem. Commun.*, 1989, 126.
9 G. M. Norante, M. Di Vaira, F. Mani, S. Mazzi and P. Stoppioni, *J. Chem. Soc., Dalton Trans.*, 1992, 361.
10 M. Di Vaira, F. Mani, M. Menicatti, P. Stoppioni and A. Vacca, *J. Chem. Soc., Dalton Trans.*, 1997, 661.
11 M. Di Vaira, F. Mani and P. Stoppioni, *Eur. J. Inorg. Chem.*, 1999, 833.
12 M. Di Vaira, F. Mani and P. Stoppioni, *Inorg. Chim. Acta*, 2000, **303**, 61.
13 M. Di Vaira, F. Mani, N. Nardi, P. Stoppioni and A. Vacca, *J. Chem. Soc., Dalton Trans.*, 1996, 2679.
14 M. Di Vaira, F. Mani and P. Stoppioni, *J. Chem. Soc., Dalton Trans.*, 1998, 1879.
15 F. Mani, R. Morassi, P. Stoppioni and A. Vacca, *J. Chem. Soc., Dalton Trans.*, 2001, 2116.
16 E. Kimura, M. Shionoya, T. Mita and Y. Litika, *J. Chem. Soc., Chem. Commun.*, 1987, 1712.
17 M. Kodera, N. Koura, S. Hosohara, M. Nishimura, M. Ohba, H. Okawa and S. Kida, *Inorg. Chim. Acta*, 1993, **214**, 97.
18 J. Costa, R. Delgado, M. C. Figueira, R. T. Henriques and M. Teixeira, *J. Chem. Soc., Dalton Trans.*, 1997, 65.
19 J. Costa, R. Delgado, M. G. B. Drew and V. Félix, *J. Chem. Soc., Dalton Trans.*, 1999, 4331.
20 J. Costa and R. Delgado, *Inorg. Chem.*, 1993, **32**, 5257.
21 J. Costa, R. Delgado, M. G. B. Drew and V. Félix, *J. Chem. Soc., Dalton Trans.*, 1998, 1063.
22 L. D. Pettit and H. K. J. Powell, *IUPAC Stability Constants Database*, Academic Software, Timble, 2003.
23 P. Gans, A. Sabattini and A. Vacca, *Talanta*, 1996, **43**, 1739.

24 L. Alderighi, P. Gans, A. Ienco, D. Peters, A. Sabatini and A. Vacca, *Coord. Chem. Rev.*, 1999, **184**, 311.
25 L. Banci, A. Bencini, C. Benelli, D. Gatteschi and C. Zanchini, *Struct. Bonding*, 1982, **52**, 37.
26 A. B. P. Lever, *Inorganic Electronic Spectroscopy*, Elsevier, Amsterdam, 2nd edn, 1984.
27 I. Bertini and C. Luchinat, *Adv. Inorg. Biochem.*, 1984, **6**, 71.
28 L. Sacconi, F. Mani and A. Bencini, *Comprehensive Coordination Chemistry*, ed. G. Wilkinson, R. D. Gillard and J. A. McCleverty, Pergamon Press, 1987, vol. V, pp. 1–137.
29 H. W. de Wijn and R. F. van Balderen, *J. Chem. Phys.*, 1967, **46**, 1381.
30 A. R. Coffino and J. Peisach, *J. Magn. Reson., Ser. B*, 1996, **111**, 127.
31 N. Niccolai, E. Tiezzi and G. Valensin, *Chem. Rev.*, 1982, **82**, 359.
32 R. Kumar and S. Chandra, *Spectrochim. Acta, Part A*, 2007, **67**, 188.
33 C. Bucher, E. Duval, J.-M. Barbe, J.-N. Verpeaux, C. Amatore, R. Guilard, L. Le Pape, J.-M. Latour, S. Dahaoui and C. Lecomte, *Inorg. Chem.*, 2001, **40**, 5722.
34 D. F. Xiang, X. S. Tan, Q. W. Hang, W. X. Tang, B.-M. Wu and T. C. W. Mak, *Inorg. Chim. Acta*, 1998, **277**, 21.
35 G. A. van Albada, A. Mohamadou, W. L. Driessen, R. de Gelder, S. Tanase and J. Reedijk, *Polyhedron*, 2004, **23**, 2387.
36 L. R. Guilherme, S. M. Drechsel, F. Tavares, C. J. da Cunha, S. T. Castaman, S. Nakagaki, I. Vencato and A. J. Bortoluzzi, *J. Mol. Catal. A: Chem.*, 2007, **269**, 22.
37 R. Kumar and S. Chandra, *Spectrochim. Acta, Part A*, 2007, **67**, 188.
38 N. Niccolai, E. Tiezzi and G. Valensin, *Chem. Rev.*, 1982, **82**, 359.
39 M. Valko, R. Klement, P. Pelikán, R. Boca, L. Dlhán, A. Böttcher, H. Elias and L. Müller, *J. Phys. Chem.*, 1995, **99**, 137.
40 M. Scarpellini, A. J. Wu, J. W. Kampf and V. L. Pecoraro, *Inorg. Chem.*, 2005, **44**, 5001.
41 A. Bencini, I. Bertini, G. Canti, D. Gatteschi and C. Luchinat, *J. Inorg. Biochem.*, 1981, **14**, 81.
42 L. Banci, A. Bencini, C. Benelli, D. Gatteschi and C. Zanchini, *Struct. Bonding*, 1982, **52**, 37.
43 J. R. Pilbrow, *Transition Ion Electron Paramagnetic Resonance*, Oxford University Press, 1990, pp. 144–149.
44 J. Zarembowitch and O. Kahn, *Inorg. Chem.*, 1984, **23**, 589.
45 A. Louati, A. Kuncaka, M. Gross, C. Haubtmann, M. Bernard, J.-J. André and J.-J. Brunette, *J. Organomet. Chem.*, 1995, **486**, 95.
46 F. Neese, *Diploma Thesis*, University of Konstanz, 1993.
47 Y. Li, *Bull. Chem. Soc. Jpn.*, 1996, **69**, 2513.
48 B. J. Hathaway, *Coord. Chem. Rev.*, 1983, **52**, 87.
49 P. Barbaro, C. Bianchini, G. Capannesi, L. Di Luca, F. Laschi, D. Petroni, P. A. Salvadori, A. Vacca and F. Vizza, *J. Chem. Soc., Dalton Trans.*, 2000, 2393.
50 K. P. Guerra, R. Delgado, L. M. P. Lima, M. G. B. Drew and V. Félix, *Dalton Trans.*, 2004, 1812.
51 V. Félix, M. J. Calhorda, J. Costa, R. Delgado, C. Brito, M. T. Duarte and M. G. B. Drew, *J. Chem. Soc., Dalton Trans.*, 1996, 4543.
52 D. F. Evans, *J. Chem. Soc.*, 1959, 2003.
53 D. D. Perrin and W. L. F. Armarego, *Purification of Laboratory Chemicals*, Pergamon, Oxford, 3rd edn, 1988.
54 R. Delgado, J. J. R. Fraústo da Silva, M. T. S. Amorim, M. F. Cabral, S. Chaves and J. Costa, *Anal. Chim. Acta*, 1991, **245**, 271.
55 *SHELX-97*, G. M. Sheldrick, University of Göttingen, 1997.
56 PLATON program, A. L. Spek, *J. Appl. Crystallogr.*, 2003, **36**, 7.